Ground Support 2023 – J Wesseloo (ed.)

doi:10.36487/ACG_repo/2325_17

Ground support assessment for a large crusher chamber

E Montiel *SRK Consulting, Chile*

V Jelicic *SRK Consulting, Chile*

E Trujillo *Nexa Resources, Peru*

E Hormazabal *SRK Consulting, Chile*

J Cabrera *SRK Consulting, Peru*

Abstract

This paper describes the stability assessment to an underground crushing chamber that presents deformations and cracks due to the proximity of stope extraction by an open stoping mining method.

According to the production plan, several stopes would be mined in sectors close to the crusher chamber. To evaluate the performance of the supports in response to the chamber, a three-dimensional numerical model was generated by finite differences method with sufficient detail to show the effects that such a mining plan could generate, including allowing alerts during stope operation, providing additional support if required and recommending other additional mitigation measurements that could be required. Through a process of calibration and ground performance validation, this three-dimensional model allowed the study of three predictive scenarios considering different mining strategies for which the criteria of strain rate and the capacity of the supports were complemented by the review of changes in the convergence product of the mining sequence.

Keywords: *ground support performance, numerical modelling, underground excavations, convergence analysis*

1 Introduction

The performance of the mine's ground support during active operations presents a challenge related to the impact of the required excavation design. According to Villaescusa (2014), although support design in most stoping operations is straightforward, rock mass conditions and induced stresses can change as the mining progresses. Factors such as increased extraction depth or surges in global extraction can lead to overstressing, resulting in a change in support performance that may be deemed unacceptable. Lorig & Varona (2013) explain that mining tunnels must accommodate complex variations in the stress field caused by mining activities, leading to challenging and extreme situations for both the tunnel and its ground support systems.

Villaescusa (2014) further suggests that the design process becomes more complex when seismicity and dynamic loads are expected, whether from a distance or directly affecting the excavation surface. Calculation methodologies for these demands have been developed by Kaiser et al. (1996) and Kaiser (2014). Additionally, Pardo et al. (2012) indicate that in cases where overstress conditions occur around the excavation, more comprehensive analyses, such as three-dimensional (3D) ones, provide greater insight into changes in rock stresses as extraction progresses. The authors even emphasise the importance of retrospective analyses for calibration and gaining field experience in mine behaviour. Vakili et al. (2013) propose a guideline for optimising support design using numerical methods, and provide a compilation of examples where modelling has been utilised to verify and validate support selection. Bahrani & Hadjigeorgiou (2018) present a case study on drift analysis influenced by 'stopes' in anisotropic conditions, allowing for the visualisation of displacements and identification of weakened sectors resulting from the extraction of each stope and their impact.

Based on the above, this document aims to provide an illustrative case that addresses the calibration requirements (through back-analysis) and their implementation for evaluating predictive scenarios. This case specifically focuses on a crushing chamber and its adjacent works in a mine located in Peru. Additionally, it encompasses knowledge in terms of the performance of the existing support system, which is integrated into the analysis. The document will determine a utility model to aid the mine in making decisions regarding the mining plan and potential actions for enhancing the current support systems operational within the mine.

2 Mine and geotechnical conditions

2.1 Relevance of the mining strategy required by the life of mine plan

The crushing chamber is situated at a depth of 300 metres, within a combination of geotechnical units consisting of orebodies and host rocks along with the presence of geological faults. Figure 1 illustrates this sector, including the nearby levels. The mine employs an open stoping method for extraction, which also encompasses areas surrounding the crushing chamber. The mining plan for the entire life span of the mine (LOM) entails the exploitation of stopes near the crushing chamber. However, this raises concerns about the operational continuity of the chamber until the final planned year of extraction.

Figure 2 depicts the planned underground workings and chambers (highlighted in red) in the proximity of the crushing chamber throughout the LOM.

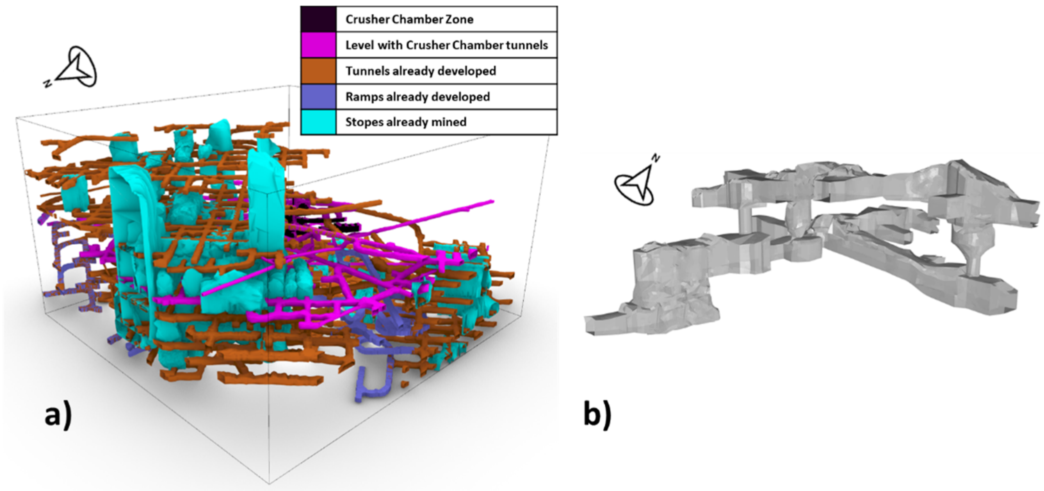

Figure 1 Existing excavations in the crushing chamber area. (a) Details of mined levels and chambers in the sector; (b) Crushing chamber area

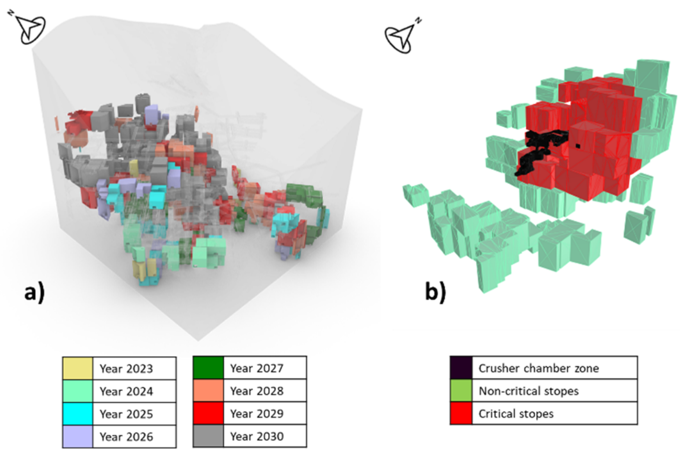

Figure 2 Planned stopes for extraction until the end of the mine's life. (a) Planned stopes for the LOM; (b) Stopes near the crushing room within a 150-m radius

2.2 3D Numerical model using finite differences method

The analysis utilised a three-dimensional model comprising a calculation box measuring 420 metres in length, 400 metres in width and 240 metres in height. The model's maximum extension was determined according to the topographic surface. Figure 3 provides a visual representation of the mesh employed, highlighting the intricate details of the topographic surface. The mesh used in this analysis explicitly incorporated underground tunnels, with a higher density of elements in the vicinity of the crushing chamber. In this sector, the element size ranged from 0.4–1.2 m, while for the remaining excavations, an element size of 2–4 m was used. Figure 3 illustrates this, highlighting the concentrated densification in the centre of the image.

Furthermore, the stopes were implicitly incorporated into the analysis, with their shape determined by the contours of the areas within each geometry, as depicted in Figure 4.

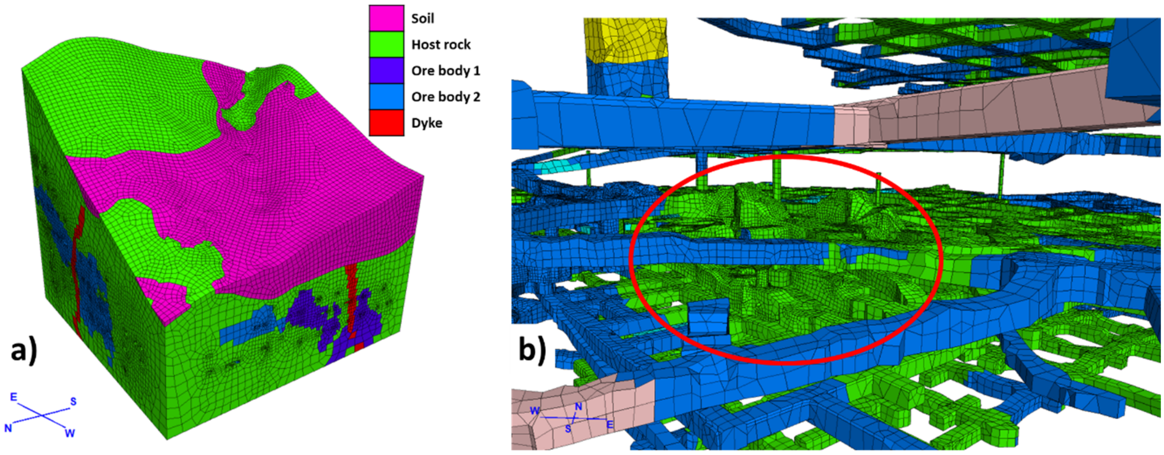

Figure 3 Mesh display of 3D numerical model and densification detail of the mesh in the crushing room sector. (a) Perspective view of model with topographic surface; (b) Detail of the mesh in the crushing zone

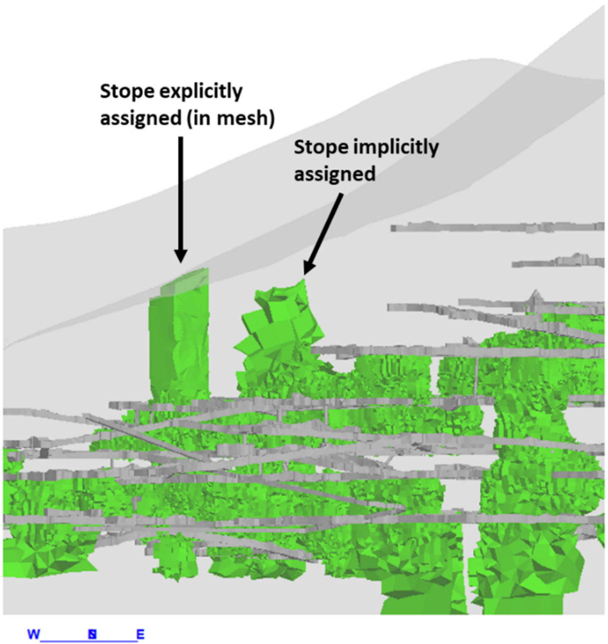

Figure 4 Allocation of stopes implicitly assigned within the numerical model

Moreover, the inclusion of the soil layer within the model mesh allows for a more detailed analysis of the contact interface. This contact between the soil and rock layers serves as a crucial factor in evaluating the potential occurrence of subsidence. It enables a thorough examination of ground behaviour and deformation, particularly in areas where geological faults intersect with the soil layer, as illustrated in Figure 5.

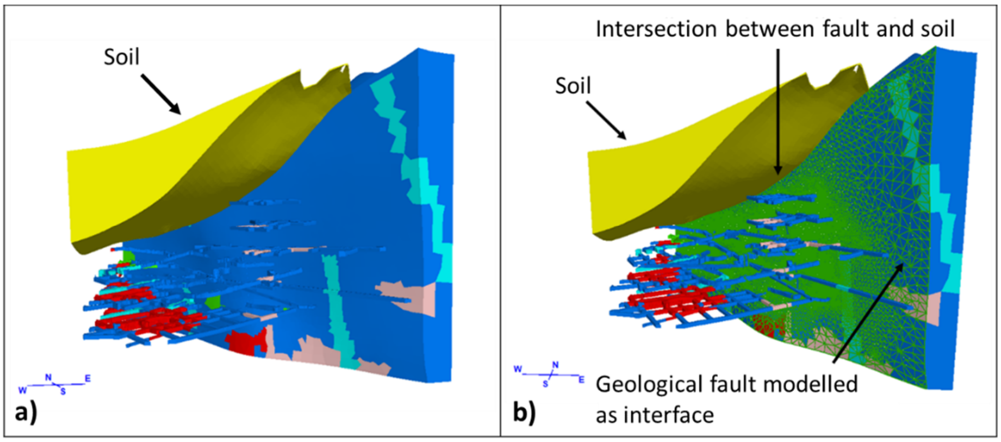

Figure 5 Incorporation of the layer in a numerical model. (a) View of the soil layer in a numerical model; (b) View of the intersection of soil with a geological fault in a numerical model

2.3 Current ground support conditions

In order to gather further detailed information about the current state of the crushing room area and the surrounding underground works, vulnerable sectors have been monitored and tracked. Visual records of these areas have been constantly updated to provide an ongoing assessment of their condition. Reactivity has been observed in proximity to the extraction of stopes, which raises concerns about the stability of these areas. Figure 6 provides a summary of the damaged sectors and presents examples of the level of damage observed.

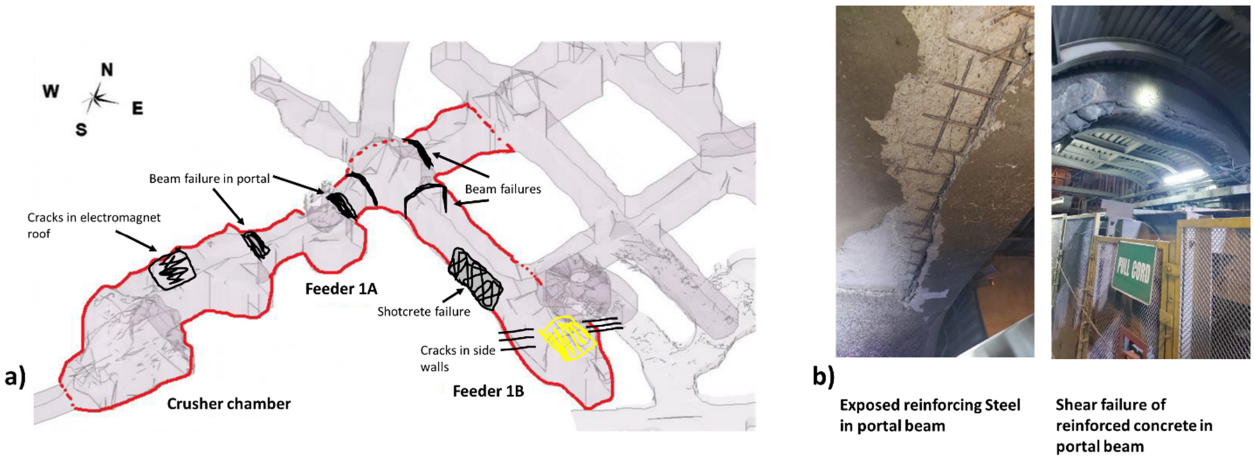

Figure 6 Monitoring of support damage in various sectors. (a) Overview of damaged sectors; (b) Photos revealing support deficiencies

2.4 Geological and geotechnical considerations of the sector

In terms of characterisation, the rock mass exhibits fair to poor quality (RMR < 55) according to the classification for the Rock Mass Rating (Bieniawski 1989). It is generally subjected to significant blasting damage, making each sector susceptible to generalised plasticity. These observations are depicted in Figure 7, which illustrates the condition closest to that experienced in the studied sector. To further investigate this condition, 3D numerical models will be utilised for detailed analysis.

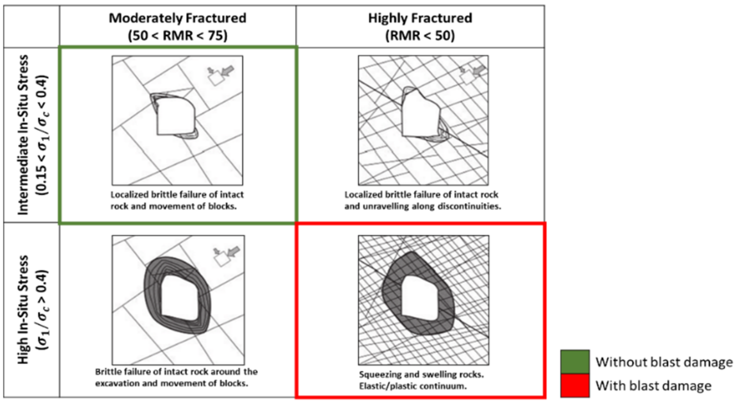

Figure 7 Failure condition classification for cases evaluated (modified after Kaiser et al. 2000)

The analysis sector consists of six characterised geotechnical units, where two of them correspond to host rocks, three to orebodies and one unit to soil. Figure 8 shows the correspondence of geotechnical units with respect to the underground tunnels surrounding the crushing room, where the crusher chamber is in host rock while the feeders are in the orebody.

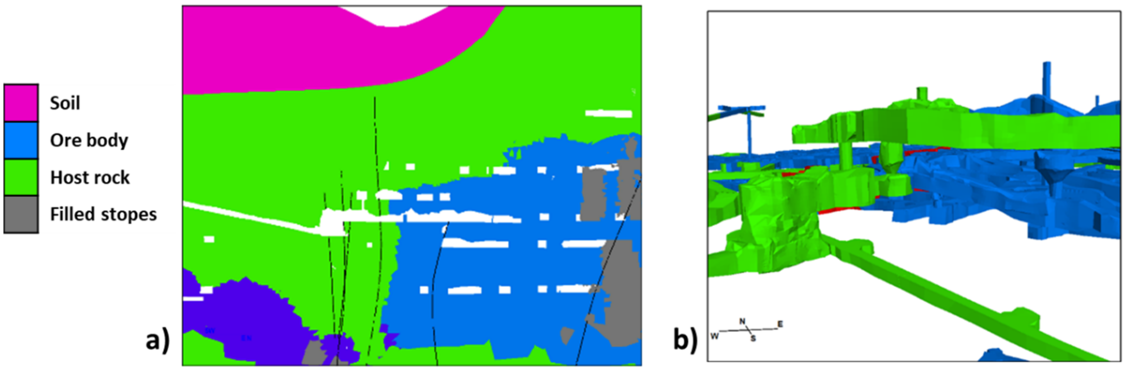

Figure 8 Geotechnical units associated with the crushing room area. (a) Section view; (b) Perspective view

Furthermore, the geotechnical mapping has revealed the presence of nine geological faults in the crushing room sector. These faults are characterised by poor infilling material and weak strength properties. The spatial arrangement of these faults is depicted in Figure 9.

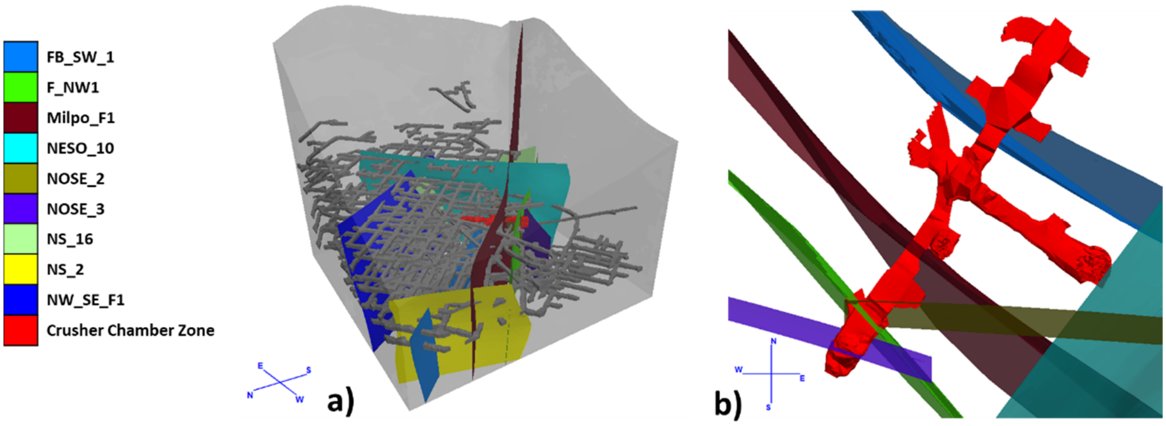

Figure 9 Geological faults in the study sector. (a) Perspective view; (b) Plan view of crusher chamber zone

3 Calibration and support condition

According to the geotechnical group that developed this study, calibration will be considered as the process of examining and adjusting the results of geotechnical characterisation in relation to its behaviour due to engineering procedures that imply modification in its stress state. This calibration covers the study and investigation of historical instabilities that allow the development of back-analysis.

In the context of the case study, an initial opportunity for calibration arose through the evaluation of historical subsidence caused by the exploitation of a stope in the vicinity of the study sector. This subsidence, which was expected to be stable according to empirical analyses, was assessed for calibration purposes. Please refer to Figure 10 for visual representation of the initial assessment carried out before its extraction.

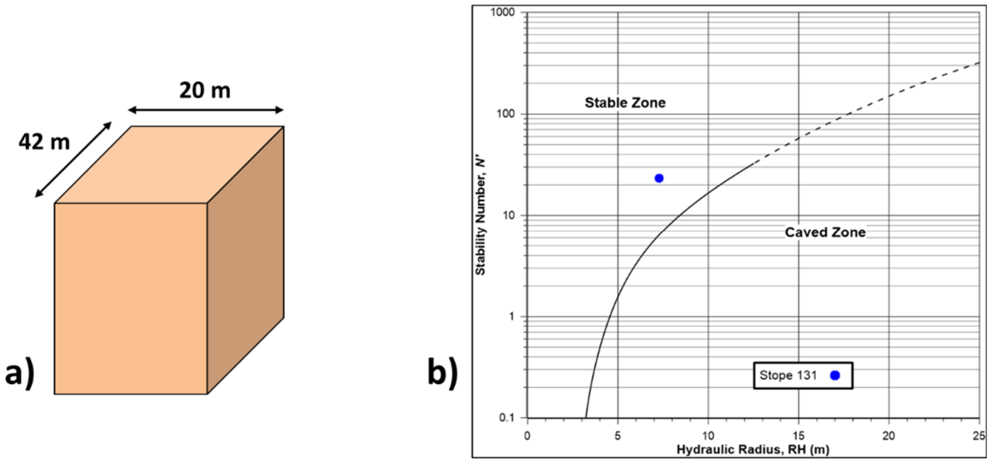

Figure 10 Empirical evaluation of the stope's crown individually. (a) View of the evaluated stope; (b) Empirical assessment of the crown

However, the studied stope was already surrounded by other previously extracted filled stopes, which shows a significant increase in the hydraulic radius of the stope crown, causing it to transition from a stable to an unstable condition as illustrated in Figure 11. This finding confirms the geotechnical parameters defined in the characterisation effectively reproducing the crown pillar failure and resulting in the propagation of subsidence to the surface. Figure 12 showcases the primary tests conducted to replicate the failure in the rock bridge present on the crown pillar of the studied stope.

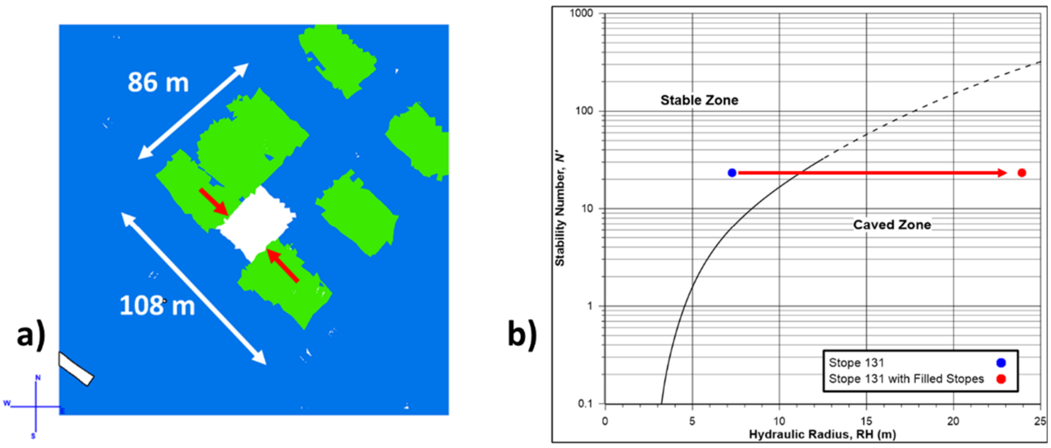

Figure 11 Empirical evaluation of the stope's crown pillar considering surrounding filled stopes. (a) Plan view of the evaluated stope with nearby backfill; (b) Empirical assessment for the stope's crown

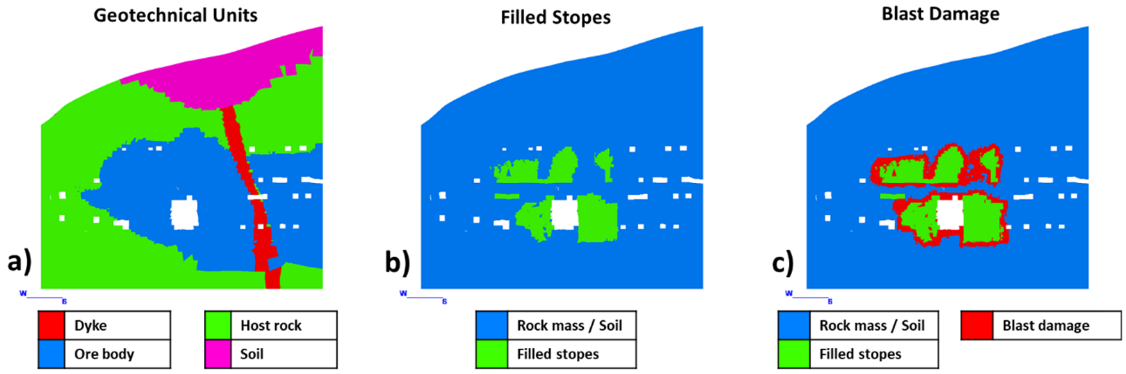

Figure 12 **Section views of rock bridge's reproduction of failure in the stope's crown. (a) Geotechnical units; (b) Location of surrounding backfilled stopes; (c) Blast damage contour**

The propagation analysis and subsequent subsidence development were achieved by evaluating the model's response to the stope's excavation in relation to physical stability. The stability level was defined through the unstable velocity detection that would later be eliminated (controlled extraction), allowing the development of the cavity and subsequently defining the subsidence zone.

Figure 13 shows the result per stage of subsidence advance from its beginning, at the crown of the stope, to the connection to the surface. These results are presented as total displacement to a perspective view (scale up to 25 centimetres), with a vertical cut to the model at the centre of the slope. A noteworthy feature of this figure is that the displacements were reinitialised by stage to visualise the effect of the advance in relative terms as the instability progressed.

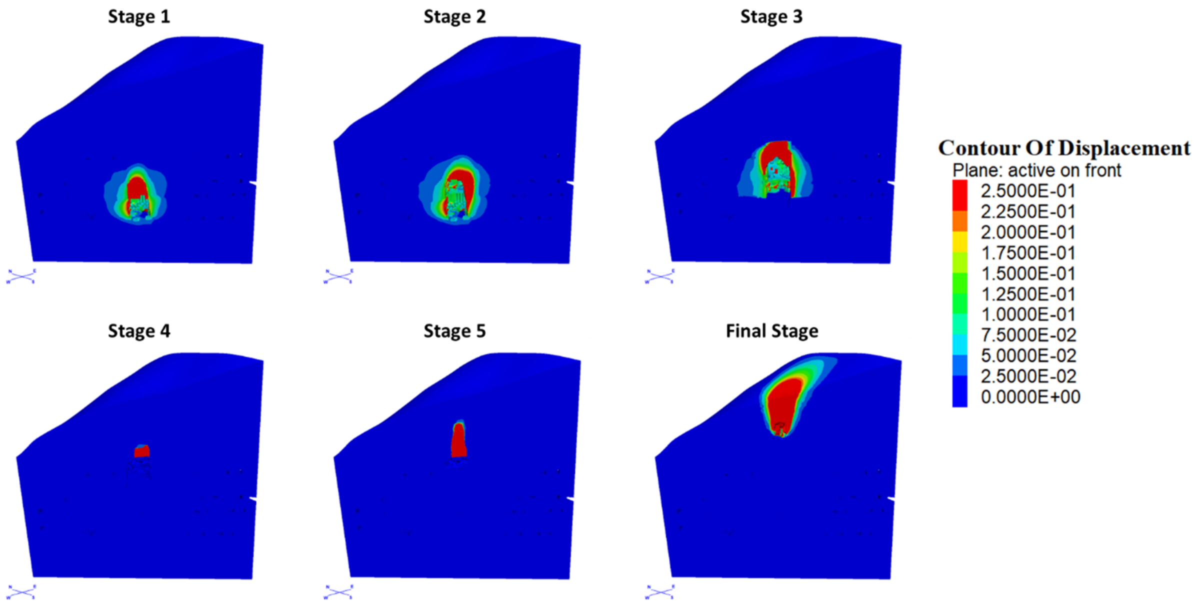

Figure 13 **Total displacement (m) view in the reproduction of subsidence propagation to the surface**

This calibration, enabled by the utilisation of advanced numerical methods, showcased the effectiveness and superiority of such approaches over traditional analysis methods in achieving the properties adjustment for the two main geotechnical units involved in the crushing room sector, as well as the optimisation of fill material properties in the stopes.

3.1 Methodology for convergence assessment

To evaluate the performance of the mine ground support in this study, the analysis of convergences and displacements due to overstress in the medium was utilised, and is described by Hoek & Marinos (2000).

This method was chosen because any significant change in its value resulting from exploitation leads to an increase in the load applied to the supports, which currently exhibit structural problems (see Figure 6).

The increment of strain in the mining sector is reaching unsustainable levels for the existing supports. Figure 14 shows the arrangement of the measurement points in the model, where a schematic tunnel section can be seen with the points located on the roof, floor and sidewalls, along with an example of the points arranged in the crushing room sector.

Additionally, measurement points were included within the rock mass at depths of 3, 6, 9 and 12 m, following the axes used for the convergence measurement points (see Figure 14). All these points were taken within the numerical model to compare different mining scenarios and their effects on the sector.

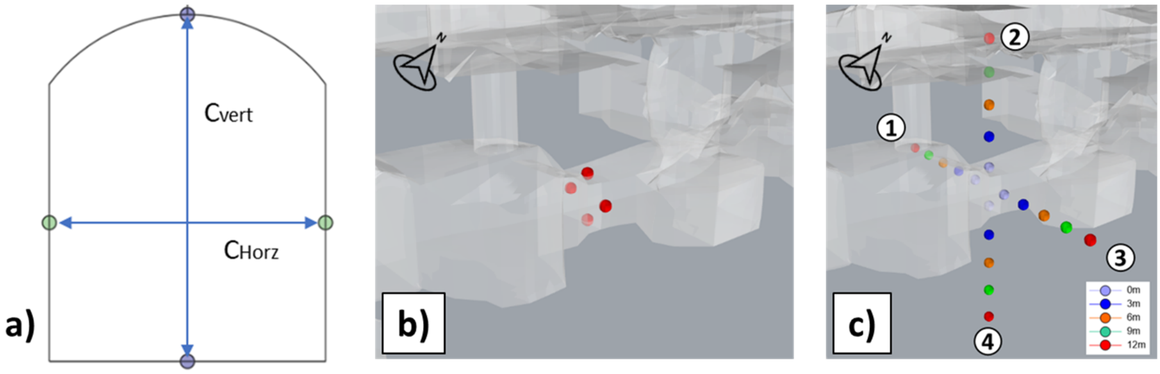

Figure 14 Points of measurement for calculation of convergence. (a) Schematic section with measurement points; (b) Example of points located on the pattern; (c) Example of points located in the rock mass

These measurements and calculations serve to evaluate both the stability of the sector and its displacement behaviour, which represents the response of the rock mass to excavation and stope extraction throughout the mine's life span. To accomplish this, 14 measuring stations were strategically placed in significant locations within this sector, as depicted in Figure 15.

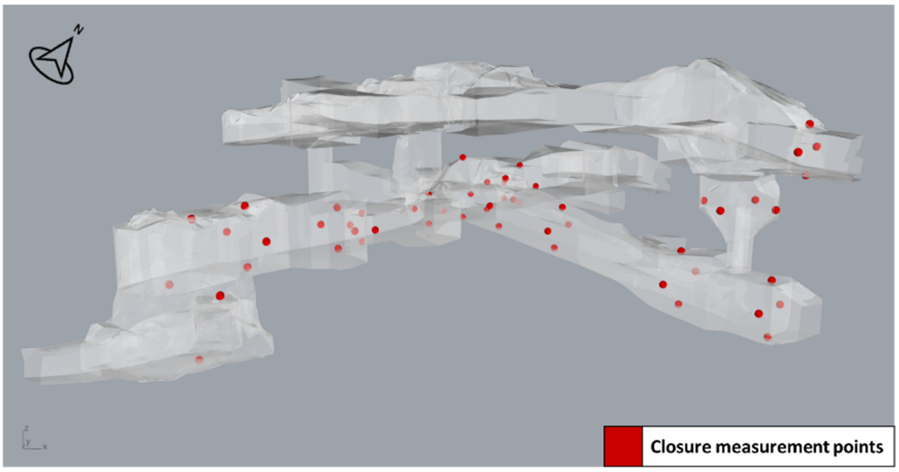

Figure 15 Convergence measurement points in the crushing area

3.2 3D support modelling

The ground support was incorporated into the model using two methods: explicit and implicit. In the explicit case, cables representing the actual installed supports were utilised, as shown in Figure 16. The figure also illustrates the sectors with different types of support, which are further detailed within the same figure. Other support elements, such as bolts, steel sets and walls, were implicitly incorporated through equivalent internal pressures along the excavation contours.

According to Hadjigeorgiou (2016), the long-term performance of the support is affected by its degradation, which needs to be examined to anticipate potential failures. This proactive approach enables the implementation of necessary rehabilitation measures to ensure its continued effectiveness. Based on the mine's records, a degradation rate of approximately 10% every 5 years was adopted, starting from the initial period of maximum strength, as depicted in Figure 17.

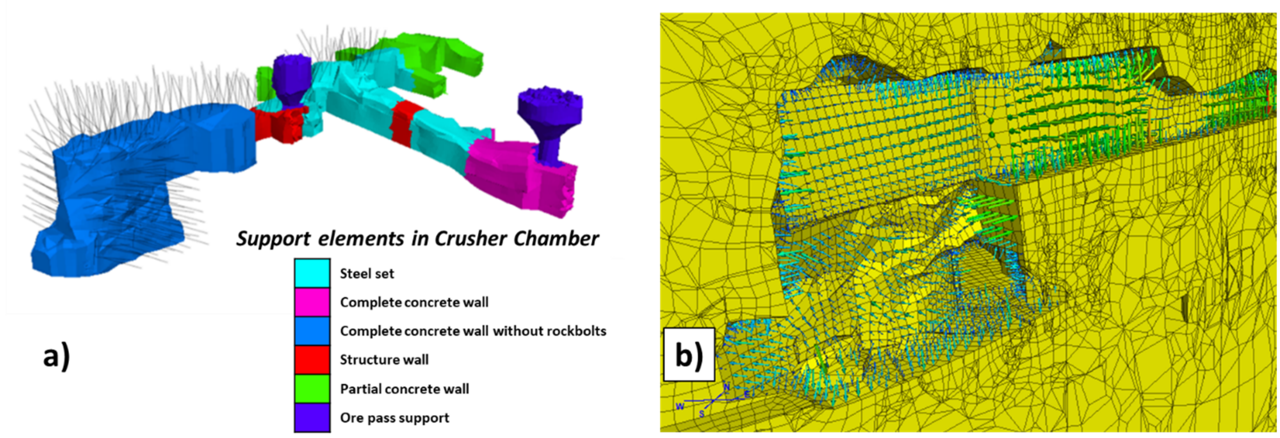

Figure 16 Modelling of supports. (a) Support zoning considered in a numerical model; (b) Application of internal pressures in a numerical model

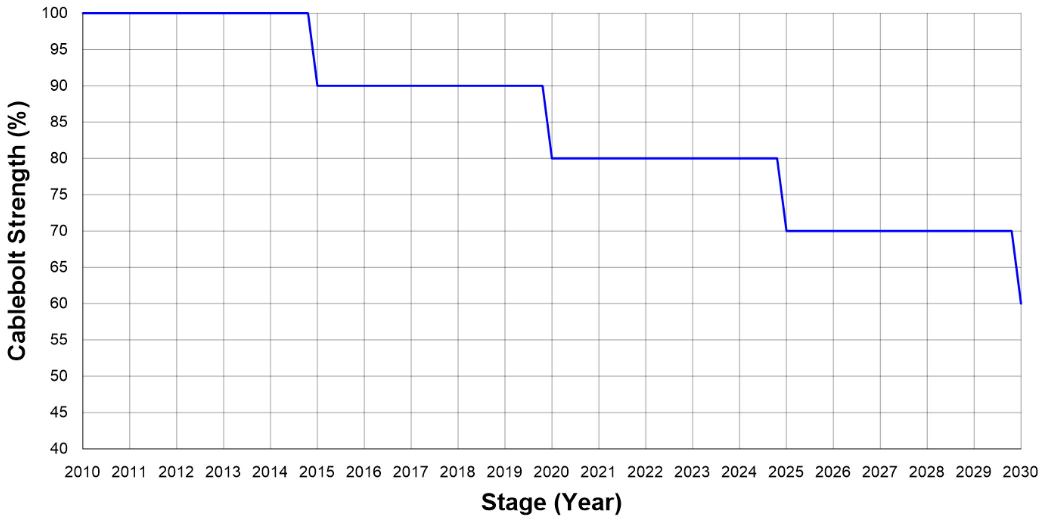

Figure 17 Cable yield strength reduction over time applied in the numerical model

4 Predictive evaluation

The objective of this analysis is to predictively assess the support capacity over the different scenarios of the mining plan. Once the model has been calibrated and the support behaviour considered, a comparative analysis was conducted among different predictive scenarios. These scenarios are described as follows:

- Base scenario: considers the complete planned exploitation, including mining all planned stopes.
- 300 m safety sphere scenario: considers partial planned mining, encompassing the excavation of stopes located outside a safety zone in the shape of a 300 m diameter sphere around the crushing room sector.
- Scenario without critical stopes: considers partial planned mining, encompassing the excavation of stopes classified as non-critical based on the results of the numerical model for the operational continuity of the crushing room sector.

4.1 Results by alternative design and comparative analysis

After reviewing the results obtained for the three evaluated scenarios, the authors conducted a comprehensive comparison of the convergences generated by mining operations in the crusher sector.

The following results are presented, differentiating between back-floor convergence and convergence in the boxes for each scenario. From the graph in Figure 18, it is evident that the mining strategy has a noticeable influence in the later years of exploitation (2028–2030), with the greatest convergence occurring in the sidewalls of the crushing room (station 1). However, the increase in convergence as the exploitation progresses is not significant, indicating that this sector is relatively insensitive to the advancement of mining operations. Conversely, the convergence results for station 2 (see Figure 19) show a distinct behaviour compared to the previous station, with values remaining close to 1% since the beginning of stope exploitation. Furthermore, an increase in convergence can be observed from the year 2025 along both the roof-floor axis and the sidewalls.

Another crucial aspect to consider in the analysis is the condition of the cables as the exploitation progresses. Figure 20 provides a comparison of the cable condition at the end of the exploitation, revealing significant differences between the two scenarios and with a more favourable condition observed in the security sphere scenario.

These results also underscore the impact of the assumed time-dependent loss of capacity of the cables, emphasising the importance of implementing robust quality control measures for the installed support systems to detect and monitor sectors with the highest demands.

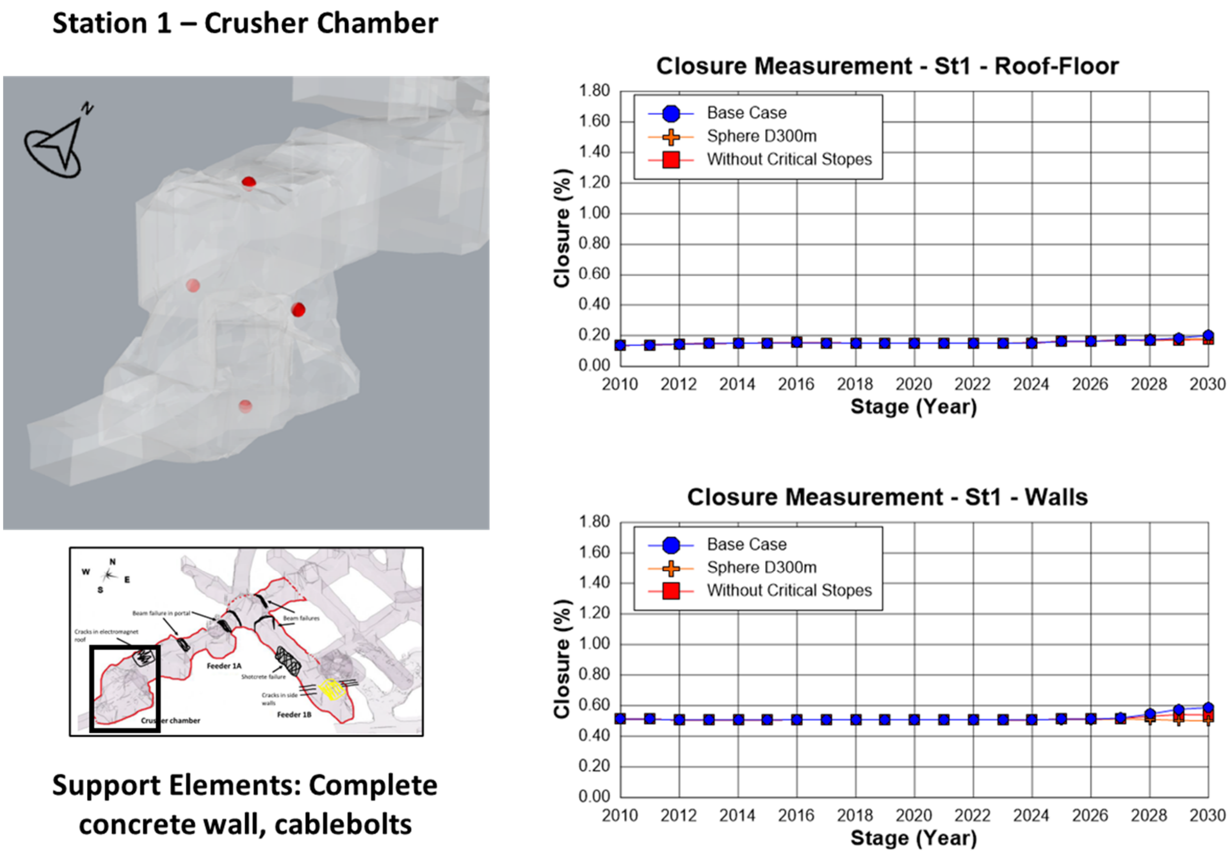

Figure 18 Convergence results at station 1

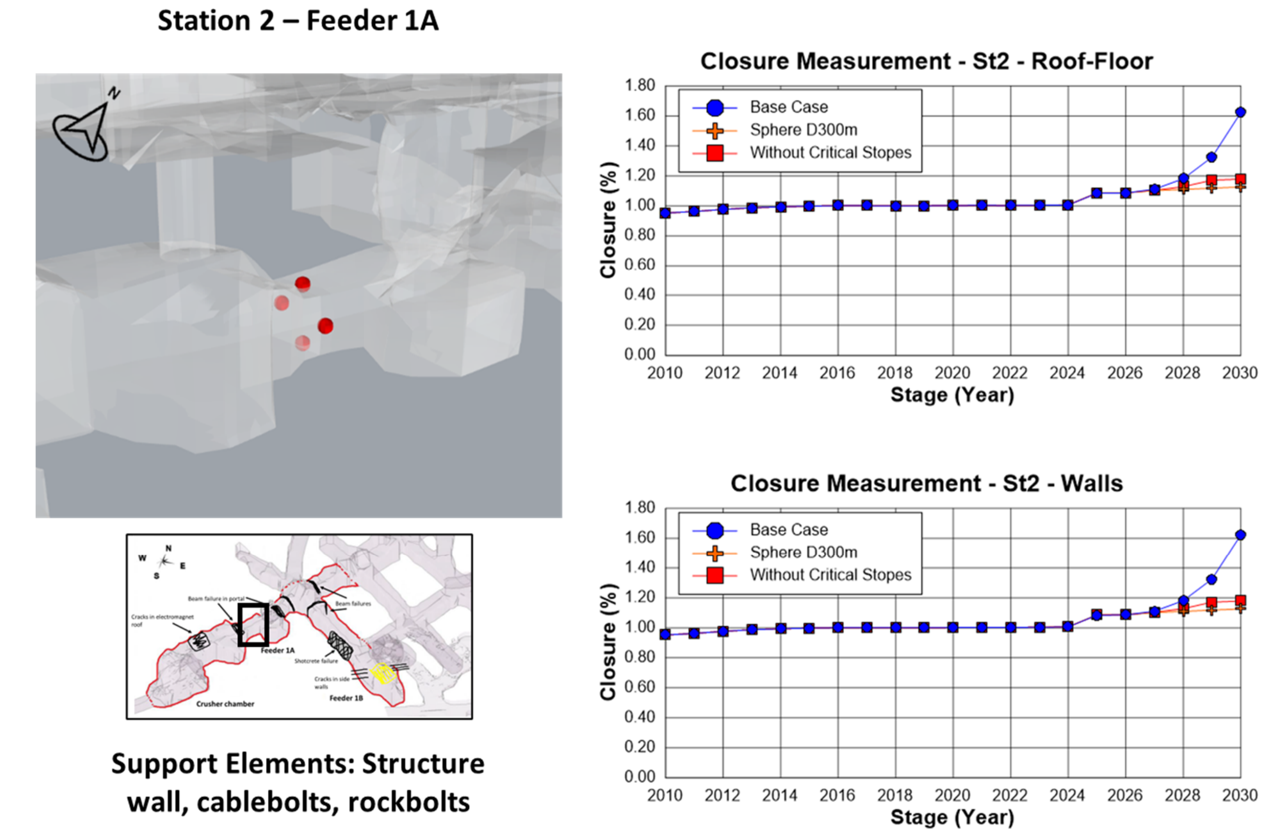

Figure 19 Convergence results at station 2

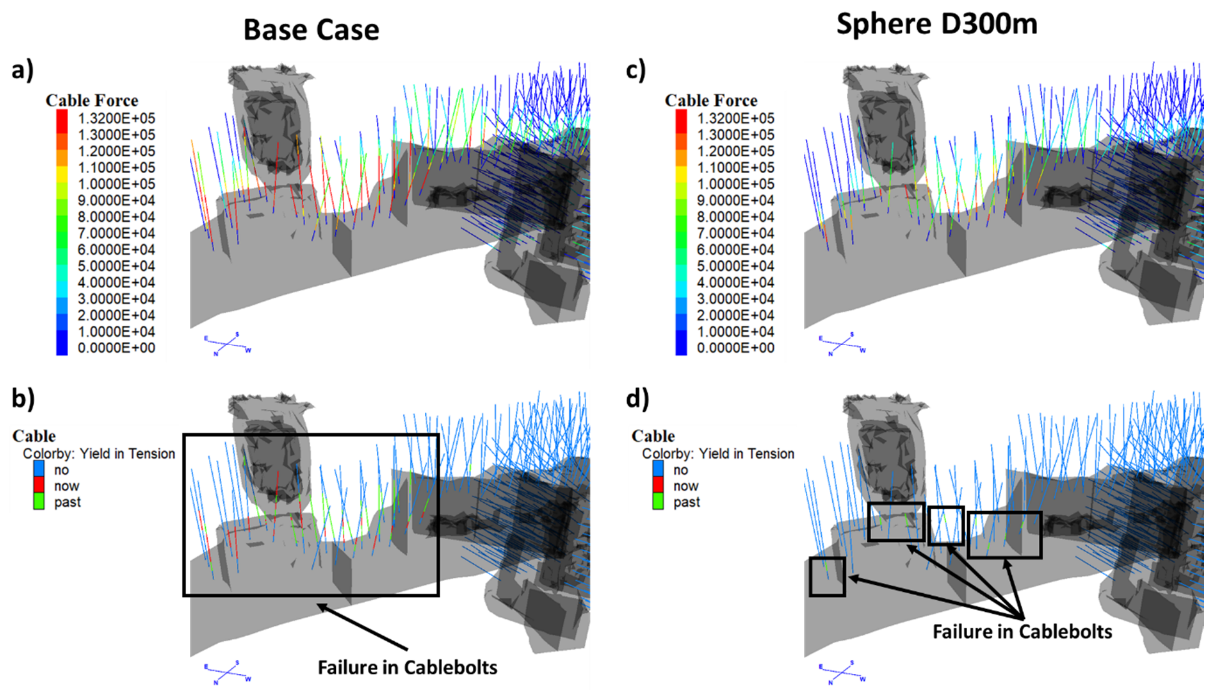

Figure 20 Axial force detail and cable condition at the end of the mining. (a) Axial force (N) in cables for the base case; (b) Condition of cables (no failure, failure at the current stage or a past stage) for the base case; (c) Axial force (N) in cables for the 300 m sphere case; (d) Condition of cables (no failure, failure at the current stage or a past stage) for the 300 m sphere case

4.2 Additional support estimate for areas vulnerable to mining

Based on the results presented earlier, the main sectors requiring reinforcement were identified in case the crusher is used until the end of mining. Reinforcement options in the form of additional support pressure were evaluated, revealing that a support pressure of 400 kPa is necessary to compensate for the loss of cable strength starting from the year 2025. However, starting from the year 2028, the effect of nearby mining becomes noticeable in the convergence of the evaluated station.

Figure 21 displays the results for the estimation of additional reinforcement required for station 2, which presented one of the worst conditions in terms of ground support. Based on the results analysed, an estimation was made for the critical period before a significant increase in convergence occurs at each of the 14 stations in the three evaluated scenarios. This estimation also includes the identification of vulnerable sectors requiring additional support.

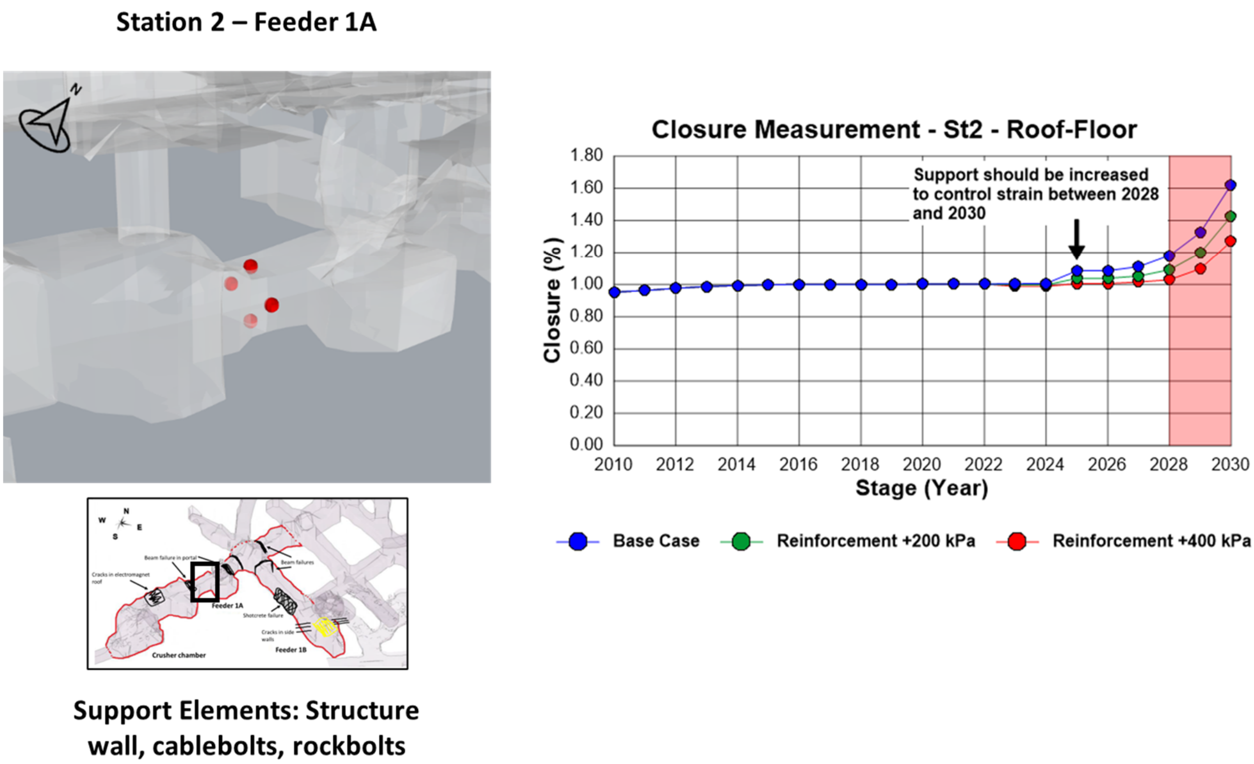

Figure 21 Convergence results with additional support application

5 Conclusion

Verifying the support condition using three-dimensional numerical models allows for a more detailed analysis, resulting in clearer results and better decision-making regarding potential rehabilitation or reinforcement for the crusher chamber. In the case of this study, the numerical model provided greater clarity on the current state of the installed support in the crushing room sector and its response to the progress of the excavation, highlighting the most vulnerable areas and estimating the necessary equivalent support for its operational continuity.

Additionally, this study allowed for the comparison of different mining alternatives that would be compatible with the continuity of the crusher, providing further guidance in mine planning to balance maximising reserve extraction while ensuring the stability of the underground tunnels required for mineral crushing.

Acknowledgement

The authors extend their gratitude to Nexa Resources for granting permission to publish this article, with special acknowledgement to John Ames for his support in the necessary coordination and his invaluable contribution during the technical development of the presented numerical evaluations.

References

Bahrani, N & Hadjigeorgiou, J 2018, 'Influence of stope excavation on drift convergence and support behavior: insights from 3D continuum and discontinuum models', *Rock Mechanics and Rock Engineering*, vol.51, pp. 2395–2413, https://doi.org/10.1007/s00603-018-1482-5

Bieniawski, ZT 1989, 'Geomechanics classification (rock mass rating system)', in *Engineering Rock Mass Classifications*, John Wiley & Sons Inc., Toronto.

Hadjigeorgiou, J 2016, 'Rock support: degradation and failure', in E Nordlund, T Jones & A Eitzenberger (eds), *Ground Support 2016: Proceedings of the 8th International Symposium on Ground Support in Mining and Underground Construction*, Luleå University of Technology, Luleå.

Hoek, E & Marinos, P 2000, 'Predicting tunnel squeezing problems in weak heterogeneous rock masses', in *Tunnels and Tunnelling International*, pp. 45–51.

Kaiser, PK 2014, 'Deformation-based support selection for tunnels in strainburst-prone ground', in M Hudyma & Y Potvin (eds), *Deep Mining 2014: Proceedings of the Seventh International Conference on Deep and High Stress Mining*, Australian Centre for Geomechanics, Perth, pp. 227–240, https://doi.org/10.36487/ACG_rep/1410_13_Kaiser

Kaiser, P, Diederichs, MS, Martin, CD, Sharp, J & Steiner, W 2000, 'Underground works in hard rock tunnelling and mining', *Proceedings of GeoEng2000*, Technomic Publishing Co, Lancaster, pp. 841–926.

Kaiser, PK, McCreath, DR & Tannant, DD 1996, *Rockburst Support Handbook*, Canadian Mining Industry Organization, Sudbury.

Lorig, LJ & Varona, P 2013, 'Guidelines for numerical modelling of rock support for mines', in Y Potvin & B Brady (eds), *Ground Support 2013: Proceedings of the Seventh International Symposium on Ground Support in Mining and Underground Construction*, Australian Centre for Geomechanics, Perth, pp. 81–105, https://doi.org/10.36487/ACG_rep/1304_04_Lorig

Pardo, C, Villaescusa, E, Beck, D & Brzovic, A 2012, 'Back analysis of intensive rock mass damage at the Teniente mine', in *Proceedings of the 2012 Australian Mining Technology Conference*, Colourwise Digital, Brisbane.

Vakili, A, Sandy, MP, Mathews, M & Rodda, B 2013, 'Ground support design under highly stressed conditions', in Y Potvin & B Brady (eds), *Ground Support 2013: Proceedings of the Seventh International Symposium on Ground Support in Mining and Underground Construction*, Australian Centre for Geomechanics, Perth, pp. 551–564, https://doi.org/10.36487/ACG_rep/1304_38_Vakili

Villaescusa, E 2014, *Geotechnical Design for Sublevel Open Stoping*, CRC Press, Boca Raton, pp. 345–346.